Multi-color complex spatial light modulation with a single digital micromirror device

HENGZHE YAN,[1] YUNCONG SUN,[1] YIQIAO LIN,[1] FEIXIANG CHU,[1] AND WENJIE WAN[1,2,*] (iD)

[1] *State Key Laboratory of Advanced Optical Communication Systems and Networks, University of Michigan-Shanghai Jiao Tong University Joint Institute, Shanghai Jiao Tong University, Shanghai 200240, China*

[2] *Department of Physics and Astronomy, Shanghai Jiao Tong University, Shanghai 200240, China*
*wenjie.wan@sjtu.edu.cn

Abstract: Spatial light modulators enabling complex light field manipulation has opened up many opportunities in biomedical imaging, holographic display, and adaptive optics. However, traditional spatial light modulators do not allow multi-color operations simultaneously due to their physical constraints, while multi-color modulations are highly desirable in many applications. To overcome this limitation, we demonstrate a multi-color spatial complex light field modulation with a single binary hologram on digital micromirror devices (DMD). This method combines several neighboring micro-mirror pixels into a giant single superpixel, in which the light field's amplitude and phase can be individually determined by internal pixel combinations, and the dynamic range of phase modulation can exceed 2π for the single wavelength. As a result, this extra phase modulation range offers an additional degree of freedom for independent multi-wavelength light modulation. Based on this scheme, multi-color light modulations have been demonstrated in a 2D plane as well as in multiple 3D holographic planes. Moreover, a dual-colored Airy beam has been realized using the same technique. These results bring complex light modulation into a multi-color regime, paving the way for practical applications in information display, imaging, and optical trapping.

1. Introduction

Manipulating light-field including both phase and amplitude enables many intriguing applications in optical imaging, laser manufacture, display, and adaptive optics. Particularly, a spatial light modulator (SLM), tailoring incident light's complex field, quickly becomes a convenient and indispensable tool for various emerging technology such as holographic display [1–24], structured beam generation [25,26], optical neural network [27], computational imaging [28–30], aberration correction [31,32] and wavefront shaping [33,34]. However, the most popular SLM, i.e. liquid crystal spatial light modulator (LC-SLM), is well-known to have a low refresh rate, greatly limiting its potential in some critical applications like adapted optics [33]. In contrast, a digital micromirror device (DMD), has a refresh rate of up to 32kHz, making it possible for those high-speed application scenes [34]. But neither LC-SLM nor DMD devices can solely support complex field modulation: LC-SLM can only operate at either amplitude or phase modes, but cannot modulate them both simultaneously. And a DMD can only modulate the amplitude field in a binary way. Special treatments can be implemented based on these SLMs for complex field modulation, including the detour phase or Lee's hologram [3~5], the error diffusion method [9~11], and superpixel method [6~8]. Among them, the detour phase method and Lee's hologram generate a grating-like aperture array, whose position and size determine output phase and amplitude respectively; The error diffusion method approximates complex amplitude with binary amplitude or pure phase, diffusing residual error to remaining pixels with a high light efficiency. However, the error diffusion method is time-consuming and its parallel computing realization is

still a complex issue. In comparison, the superpixel method combines several neighboring pixels into one superpixel, in which amplitude and phase information depends on pixel combination. For each target complex amplitude, one can find a superpixel with minimum error from the target by searching exhaustively all possible pixel combinations. In this manner, amplitude and phase modulation can be achieved simultaneously in a DMD, however, for only one color.

To realize multi-color complex light field modulation is highly demanded, for example, for color holographic 3D display. Color holographic display requires modulation of three colors including Red, Green, and Blue. One convenient way named spatial multiplexing is to modulate the three colors individually with three SLMs and then combine them into a single beam [12]. However, this method is expensive and makes the system bulky, and the result is still not ideal mainly due to a small misalignment of different SLMs. Modulating multiple wavelengths with a single SLM can be mainly implemented with three techniques: the time-division method [15~17], the space-division method [18], and the depth-division method [20~21]. Here time-division method illuminates the SLM with Red, Green, and Blue light in a time sequence, as long as the refresh rate is high enough, the human eye cannot distinguish them. This method decreases the refresh rate and requires additional synchronous devices such as an electronic shutter or modulated light sources. The space-division method displays a superposition of multiple holograms calculated for different colors. It is not directly applicable to DMD or other binary modulators since it requires superposition. The depth-division method designs holograms via iterations so that the desired image can be projected at a certain plane, but cannot realize multi-plane or 3D holographic projection [1]. Another interesting technique is to utilize the full phase modulation range exceeding 2π as an additional degree for multiple wavelength modulation, this was first demonstrated in diffraction optical element (DOE) [22,23] and later in LC-SLM [24]. However, to our knowledge, none of the prior works up to now explored simultaneous multi-color complex field modulation in a single DMD.

In this work, we generalize the superpixel method previously proposed [7] to a multi-wavelength version that can modulate three-wavelength light simultaneously using DMD. For the target color light field, a binary hologram is constructed and displayed on DMD. Similar to previous work in LC-SLM [24], the basic idea is to provide a phase modulation range exceeding 2π. We demonstrate its application in 3-color holographic projection and dual-color structured beam generation. For each target complex amplitude, only a single binary hologram is displayed on a single DMD, which is different from time-multiplexing method that displays holograms in sequence, or spatial multiplexing methods that need multiple DMDs. The structure of this paper is as follows: in the second part, we introduce the principle of the multi-wavelength superpixel method; In the third part, we present examples of 3-color holographic projection and beam generation using this method; At last, we briefly discuss some detailed methods and limitations of our method, as well as potential applications.

2. Superpixel method

Our setup is shown in Fig. 1. (a). Coherent light beams illuminate the DMD and the incident directions are set such that light would be reflected along DMD's normal direction if all micromirrors are "on". The modulated optical field is then imaged and filtered by a 4f-like system, which is different from typical 4f systems in that the optical axes of the two lenses are shifted from each other. The first lens is to optically Fourier transforms the field. In Fourier plane, only particular spatial frequency components are selected to pass through the circular aperture. Meanwhile, the zero spatial frequency components, namely 0th order diffraction, are blocked together with other unwanted components. Then the light field is inversely Fourier transformed to the image plane by the second lens. The position of the aperture is (a, −Na) with respect to the 0th diffraction order, where a = $\lambda_0 f / N^2 d$, λ_0 is a reference wavelength to be set, f is the lens focal length, N is the pixel number of superpixel in one direction, and d is the DMD pixel pitch.
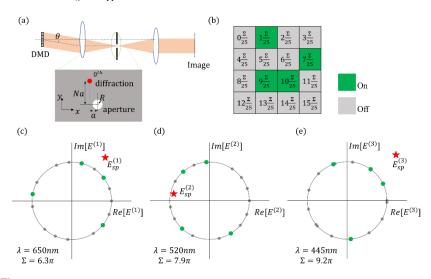
The aperture position set is similar to the previous superpixel setup, only different in that λ_0 is a parameter to be set instead of light wavelength [7]. With such aperture position, the light arriving aperture center from different DMD pixels has a phase difference. For neighboring pixels in the x direction, the phase difference is $\Delta\phi_x = \frac{\lambda_0}{\lambda}\frac{2\pi}{N^2}$, and for y direction, $\Delta\phi_y = -\frac{\lambda_0}{\lambda}\frac{2\pi}{N}$. Thus, inside a superpixel formed of $N \times N$ pixels, by turning on different DMD pixel individuals, we can get $N \times N$ equally spaced phase shifts in the range $[0, 2\pi\lambda_0/\lambda]$. And for one superpixel, the total complex amplitude of light with wavelength λ is the summation of the response of all pixels in "on" state, namely:

$$E_{sp}(A; \lambda) = \Sigma_{q=0}^{N-1}\Sigma_{p=0}^{N-1} A_{q,p} \exp[j(p\Delta\phi_x - q\Delta\phi_y)] \tag{1}$$

where A is an $N \times N$ matrix whose element $A_{q,p}$ represents state of the DMD pixel in column p and line q inside superpixel. $A_{q,p} = 1$ if the pixel is "on" and $A_{q,p} = 0$ if the pixel is "off". Equation (1) can be simplified by resorting the indexes to one dimension:

$$E_{sp}(A'; \lambda) = \sum_{n=0}^{N^2-1} A'_n \exp\left[jn\frac{\Sigma(\lambda)}{N^2}\right] \tag{2}$$

where $n = p + Nq$, $A'_n = A_{q,p}$, $\Sigma(\lambda) = 2\pi\lambda_0/f$ is the phase modulation range.

Fig. 1. Principle of the multi-color super-pixel method. (a) the 4f-like system diagram. (b) an example of 4×4 superpixel, with four pixels "on" and others "off". (c, d, e) the resulting complex amplitude of the superpixel in (b) for three wavelengths: 650nm, 520nm, 445nm.

Note that since Σ is a function of λ, the same DMD pixel combination yields different complex amplitudes for different wavelengths. As an example, we turn on four pixels in a 4×4 superpixel (Fig. 1.(b)). Then the total complex amplitude is calculated using Eq. (2) for different wavelengths, as shown in Fig. 1.(c~e).

Compared with the previous monochromatic superpixel scheme [7,11], there are some issues to take care of in our experiment. Firstly, we have an additional parameter: reference wavelength λ_0. If we set $\lambda_0 > \lambda$, then $\Sigma > 2\pi$. Such extended phase modulation range can be used for multi-wavelength modulation, as demonstrated previously for LC-SLM. And to reduce the crosstalk between different wavelengths we should choose a larger λ_0 to increase the phase modulation range Σ. However, larger λ_0 also requires a larger superpixel size to satisfy the Nyquist sampling condition, which would decrease image resolution. The tradeoff between low crosstalk and high resolution is discussed in detail in Sec.4.1. In this work, we choose 10×10 superpixel and

$\lambda_0 = 2.05\mu m$, for complex amplitude modulation of three light beams with wavelength 0.65 μm, 0.52 μm and 0.445 μm.
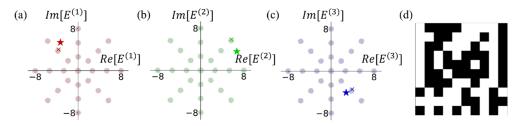
Similar to [7], a LUT is needed to connect superpixels to their complex amplitudes. However, inside a 10×10 superpixel, we have a huge number ($2^{100} \approx 10^{30}$) of pixel combinations. So, the method of exhaustion of all combinations used previously is impossible due to time and storage limits. Instead, we discretize the space of the target complex amplitude sparsely. For each target complex amplitude, the optimal superpixel can be obtained by minimizing the error between its complex amplitude and the target. The minimization problem can be expressed as:

$$\min_{\boldsymbol{A'}} f(\boldsymbol{A'}) = \sum_{all\ \lambda} \left\| E_{sp}(\boldsymbol{A'};\lambda) - E_{tar}(\lambda) \right\|^2,$$
$$\text{s.t.A'}_n = 0\ or\ 1, n = 0, 1, \dots, N^2 - 1. \tag{3}$$

where $E_{sp}(\boldsymbol{A'};\lambda)$ is the complex amplitude resulted from superpixel represented by the binary vector $\boldsymbol{A'}$ [Eq. (2)], and $E_{tar}(\lambda)$ is the target. Viewing $\boldsymbol{A'}$ as the chromosome and the error $f(\boldsymbol{A'})$ as fitness, the minimization can be done using Genetic algorithm, realized using the MATLAB toolbox [35].

All those optimal superpixels and their resulting complex amplitude are stored as a discretized look up table (DLUT). Then for arbitrary complex amplitude needed, we can search the DLUT to find the nearest available one and the corresponding superpixel. And the more finely we discretize the complex amplitude space, DLUT will contain more available superpixel and we will get higher accuracy. But it will also take more time to get the DLUT. Considering those, we discretize the amplitude in 2 bits and phase in 3 bits for each wavelength. As we'll see in Sec. 3, such accuracy is enough to get satisfying results in many applications. And it takes about 20 minutes to generate the DLUT, using a MATLAB program [35] on a personal computer. The personal computer is equipped with Windows 10 system, Intel Xeon CPU E5-4650 at 2.70 GHz, 8 cores, 16Gb of RAM memory.

The generated DLUT should contain $2^{3\times(2+3)} = 32678$ superpixels and their result field. For visualization, we project the field from 6-d space of the complex field into the complex planes of three colors respectively, as plotted in Fig. 2(a~c). Once we get the DLUT, for an arbitrary target complex amplitude, we can always search the nearest one to it. An instance of target and searched optimal available complex amplitude are marked in Fig. 2(a~c). The corresponding superpixel is shown in Fig. 2(d). After employing the searching process for all complex amplitudes of the light field, one binary hologram is generated and can be displayed on DMD. Our searching algorithm is the KD-Tree algorithm, which is suitable for simultaneous searching of multiple target complex
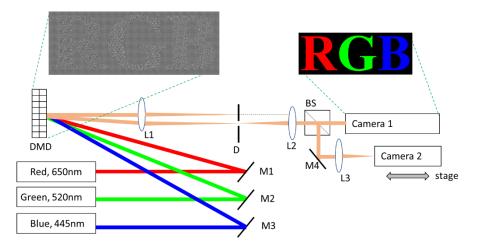

Fig. 2. (a, b, c) The DLUT projected in complex planes of the three colors. (a): red, (b): green, (c): blue. Amplitudes for each color are discretized in 2 bits, phase in 3 bits. An instance of target field: $[E^{(1)}, E^{(2)}, E^{(3)}] = [-3.3 + 5.4i, 6.7 + 3.6i, 2.8 - 4.1i]$ is projected to the three planes, marked as "star" in (a, b, c). The optimal available complex amplitude in DLUT is marked as "×". (d) Superpixel corresponding to the optimal available complex amplitude.

amplitude. The algorithm is realized using MATLAB. It takes about 0.2s to generate the binary hologram from a 200×100 pixel image on the computer mentioned above.
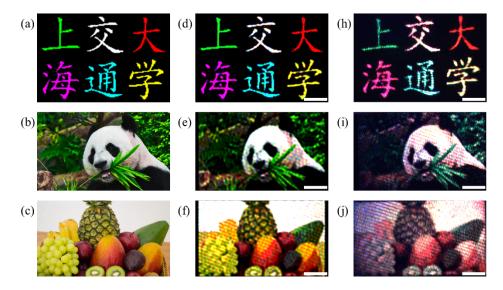
3. Experiments

We validate our method with the experimental setup shown in Fig. 3. Three laser beams in red, green, and blue color, illuminate the DMD from different angles. The incident angle differences are finely adjusted by mirrors to counteract the grating dispersion of DMD, so that three beams would be reflected through DMD's normal direction when all micromirrors are "on". This alignment process could be simplified based on the reversibility of light rays, by combining the three beams first and illuminating the DMD from desired output direction to determine mirrors (M1, M2, M3) position and orientation. After that, a hologram is displayed on DMD. The modulated light field is filtered with the 4f-like scheme as introduced in Sec. 2, where the first lens' optical axis is along DMD's normal direction. A beam-splitter splits the light beam and two cameras are used for recording light intensity both in real space and Fourier space. The two cameras are put in two translation stages along the optical axis to record light intensity at different positions.

Fig. 3. Experimental setup. The light sources are three laser diodes connected with single mode fibers and collimated lenses (Beijing Lightsensing Tech. Red: LSFLD650-3-SMFP, Green: LSFLD520-3-SMFP, Blue: LSFLD450-3-SMFP). Lasers illuminate the DMD (DMD from Shanghai VisionFly: DLP VisionFly6500, resolution 1920×1080, pixel pitch 7.56μm, binary refresh rate 9.5kHz) from different incident angle. The field modulated by DMD is then imaged and filtered by a 4f-like system composing of two achromatic lenses, L1(Daheng: GCL-010641, f = 250mm, ϕ40mm), L2(Daheng: GCL-010604, f = 100 mm, ϕ25.4mm), and diaphragm D (radius 0.4mm). Two cameras (Hikrobot: MV-CE060-10UC, colored, CMOS sensor: Sony IMX178) record the image in real space and Fourier space, respectively. The lens L3 (Daheng: GCL-010641, f = 250mm, ϕ40mm) is to optically Fourier transform the output light field to Fourier space. M1, M2, M3, M4: Mirrors; BS: Beam splitter.

We first test multi-color intensity modulation with our method. We set the intensity of the target field to be three pictures shown in Fig. 4.(a, b, c), and the phase is set to be 0. The pictures, denoted as "Chinese Characters", "Panda", "Fruits", are all rescaled to the same size of 192×108 to match our 1920×1080 DMD. For each picture, one binary hologram is generated. Then simulation is done in 3 steps for input binary hologram: fast fourier transform (FFT), digital
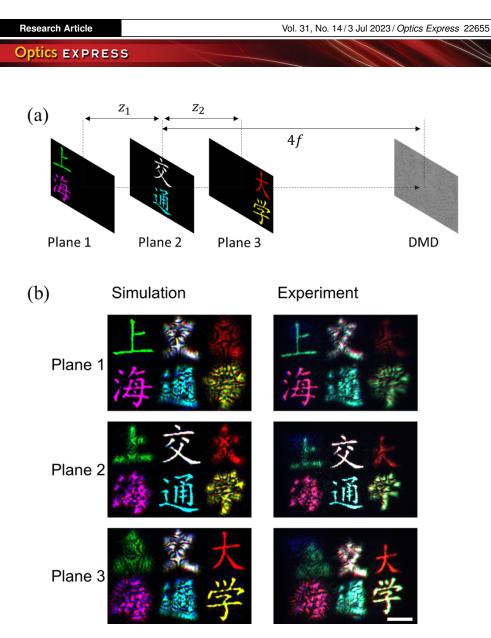
filtering according to the position and size of the diaphragm, and Inverse FFT. The simulation results shown in Fig. 4.(d,e,f) indicate that our method works perfectly for simple pictures such as "Chinese Characters". For pictures with more high spatial frequency components, such as "Panda", "Fruits", it still works well basically, though some detail losses due to filtering and there are some fringes since unwanted frequency components are not totally filtered out by diaphragm. In the experiment, the binary hologram is displayed on DMD, and the output image is recorded by camera put in the image plane of the 4f-like system as illustrated in Fig. 3. The experiment results shown in Fig. 4.(h,i,j) agree well with simulation, excerpt color distortion due to misalignment of three laser beams. Color impurity of lasers, e.g. 520nm is not purely green in the image captured by our camera, also results in such color distortion.

Fig. 4. 2D Intensity modulation. (a, b, c): original pictures: "Chinese Character", "Panda", "Fruits", (d, e, f): corresponding simulation results, (h, i, j): experimental results. Scale bar: 1 mm.
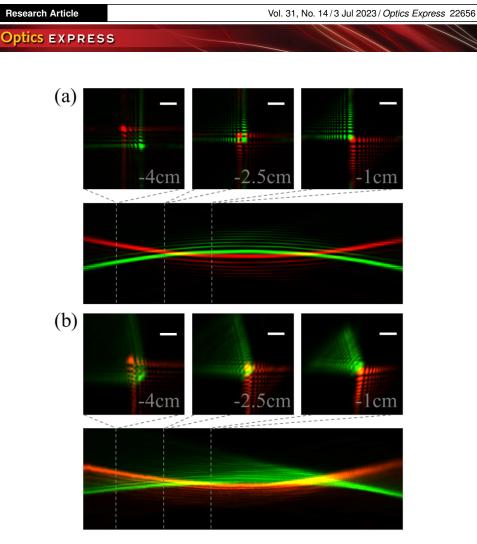
We then test the complex amplitude modulation and its application in 3-color holographic projection. As shown in Fig. 5.(a), a picture is separated into 3 panels, expected to be on focus in plane 1, plane 2, and plane 3, respectively. The field of the image plane of the 4f-like system is then the superposition of the Fresnel diffraction field of all three planes. A binary hologram is then generated using the multi-color superpixel method. In the simulation, the output field is calculated through FFT and digital filtering for the binary hologram. And light field at plane 1~3 is then calculated based on the Fresnel diffraction formula in Fig. 5(b). For the experiment, the camera moves along the optical axis and records images at those planes as shown in Fig. 5(b). Both simulation and experiment results are as expected in that for each plane, only one panel is in focus and clear while the other two panels are blurred, which indicates that our method can realize complex amplitude modulation and holographic projection. In our experiment, the target phases of panels in each plane are set to 0, which helps observe the propagation of the light field while causing relatively large crosstalk between different planes. For more practical purposes, such crosstalk can be suppressed using various methods such as adding random phases [36] or scattering medium [37].

Finally, we demonstrate the utilization of our method in multi-wavelength structured beam generation via an example of dual color Airy beam. The conventional way to generate an Airy beam is to incident a Gaussian beam into an SLM or DOE with a cubic phase profile and then conduct a spatial Fourier transform via a lens. And the phase profile can be only applied

Fig. 5. Multi-plane 3D holographic projection. (a). model diagram: three panels are expected to be projected to three planes with a single binary hologram on DMD through the 4f-like system (not shown), $z_1 = z_2 = 40mm$. (b). Simulation and experimental results: images recorded at the three planes. Scalebar: 1 mm, for all images.

for a single wavelength at one time. Our method, however, can modulate multi-wavelength simultaneously. For demonstration, we generate a dual-color Airy beam that green and red Airy beam accelerate in the opposite direction. Since only two wavelengths are modulated, we choose a smaller superpixel with 7×7 pixels and reference wavelength $\lambda_0 = 1.4\,\mu m$. Two fields with opposite cubic phase profiles, in red and green color, synthesize to one binary hologram. In the simulation, the field at the image plane of the 4f-like system is calculated as before, and then digital Fourier transformed to obtain the field at the focal plane. The field at different distances from the focal plane is then calculated based on the Fresnel diffraction formula. Three sections, with distances $-4cm$, $-2.5cm$, $-1cm$ are shown in Fig. 6.(a). And the beam trajectory is also shown in Fig. 6.(a). The experiment is done by recording images near the focal plane by moving camera along the optical axis, and the result is shown in Fig. 6(b). The main features of the Airy

Fig. 6. Dual-color Airy beam. (a). Simulation results. Top panel: Cross-section image at different positions (−4cm, −2.5cm, −1cm relative to focal spots of Fourier lens L3 (Fig. 3), where minus signs mean the positions are in front of focal spots). The image size is 1.2mm and scalebar is 200 μm. Bottom panel: parabolic trajectory image constructed by combining diagonal pixels of all cross-section images from position −5cm to 5cm in step 0.2mm. So, the trajectory image's size is 10cm in the longitudinal direction and 1.7mm in the transverse direction. (b) Corresponding experimental results.

beam, including diffraction-free and accelerating trajectory, emerge obviously in simulation and experiments.

4. Discussion and conclusion

4.1. Parameters set

There are several parameters to be set in our experiments: light wavelengths, reference wavelength λ_0 and superpixel size N. Light wavelengths are usually pre-determined by, e.g. desired light color and available lasers, while λ_0 and N are to be set. As in Sec.2, the dynamic phase modulation range for wavelength is $\Sigma = 2\pi\lambda_0/\lambda$. And phase range exceeding 2π is the key point in our method, also in previous work with LC-SLM [24]. Only when $\Sigma \gg 2\pi$ would it be possible to modulate different wavelengths independently. Namely, we should increase λ_0. Meanwhile, to increase resolution, we should decrease superpixel size N.

However, to satisfy the Nyquist sampling condition, λ_0 and N cannot be modified arbitrarily. Firstly, supposing that the target field is a constant, then the central diffraction angle in the y direction is $\theta_y = Na/f$, where $a = \lambda_0 f/(N^2 d)$. Angle in x direction is not crucial here since it is much smaller. Then the corresponding spatial frequency is $f_y = \theta_y/\lambda = \lambda_0/(\lambda N d)$. According to the Nyquist sampling theorem [38], the maximum allowed spatial frequency of the DMD with pixel pitch d is $f_{max} = 1/2d$. Therefore, $f_y < f_{max}$, yielding: $N\lambda/\lambda_0 > 2$. Next, we include the spatial frequency of target field, whose maximum spatial frequency restricted by the circular aperture is: $f_E = R/\lambda f$. Then $f_y + f_E < f_{max}$. Defining $\eta = R/a$, we have $\frac{\lambda_0}{\lambda N d}\left(1 + \frac{\eta}{N}\right) < \frac{1}{2d}$, namely:

$$\frac{N^2}{N + \eta}\frac{\lambda}{\lambda_0} > 2 \qquad (4)$$

So, to satisfy this criterion, there will be a tradeoff between high resolution (decreasing N) and low cross-talk (increasing λ_0). In our three-color modulation experiments, we set N = 10, $\eta = 0.6$, $\lambda_0 = 2.05\,\mu$m, and $\lambda = 0.445$ for blue light, then $N^2\lambda/(N + \eta)\lambda_0 = 2.04$ is slightly larger than 2.

4.2. Light coherence requirements

In general, our approach works only for spectral and spatial coherent light sources, e.g. lasers with single mode output. Spectral incoherence causes both grating dispersion due to DMD itself and dispersion due to the hologram. The former one is large but could be eliminated, e.g. by compensation with the dispersion of an additional grating [39]. The latter is smaller and its influence in single-color superpixel setup is evaluated in [7], similar for our multi-color setup. According to Sec.2, the phase difference along y direction is $\Delta\phi_y = -\frac{\lambda_0}{\lambda}\frac{2\pi}{N}$, and the phase difference along the x is unimportant here since it is much smaller. If we change wavelength slightly by $\delta\lambda$, the phase difference also changes slightly: $\delta\Delta\phi_y \sim \Delta\phi_y\delta\lambda/\lambda$. Such phase change causes dispersion and thus focused spot in the diaphragm plane moves by $\delta y \sim Na\delta\lambda/\lambda$. If we care about output in Fourier space, then the phase difference change caused by wavelength change should be small ($<\pi$) along a relatively large range (e.g. 100 superpixels). So, the bandwidth requirement is $100N\ \delta\Delta\phi_y < \pi$, which yields: $\delta\lambda < 0.005\lambda^2/\lambda_0$, typically several nanometers. However, if one only cares projected image in real space, the requirement is much loose since the image would not have significant change until focus spot moves out of the diaphragm aperture. So, the requirement is $\delta y < R$, namely $\delta\lambda < R\lambda/Na$, typically tens of nanometers.

The requirement of spatial incoherence would be similar. Spatial incoherence broaden light focusing spot, which would severely blur the output in Fourier plane. But if one only cares about the projected image in real plane, blur in Fourier plane would have little influence.

4.3. Limitations

Our method has mainly two limitations. The first is relatively low resolution due to the large superpixel size. The superpixel size is 10×10 for three-color modulation and 7×7 for dual-color modulation, larger than 4×4 for single-color modulation in previous works. We select such large size to satisfy the Nyquist sampling condition as discussed in 4.1. The second is low modulation efficiency since most light are blocked by the diaphragm. Currently, calculated light modulation efficiency is about 0.6% for three-color modulation and 2% for dual-color modulation, lower than 10% in single-color superpixel [7]. The measured light efficiency would be smaller considering DMD diffraction loss, varying with different wavelengths. To increase modulation efficiency, one could slightly increase the maximum amplitude when generating the DLUT shown in Fig. 2, though this would decrease fidelity. In addition, since the error diffusion method is known to have larger modulation efficiency than the superpixel method for single-color modulation [11], its generalization to multi-color modulation deserves further investigation.

4.4. Conclusion and outlook

Our demonstrated method allows multi-wavelength spatial light complex amplitude modulation with a single DMD. This method converts the light field of multiple wavelengths to a binary hologram displayed on DMD. Once the binary hologram is obtained, the refresh rate will be only limited by that of DMD, about 9kHz for the current DMD. We demonstrate its application in 3-color holographic projection and structured beam generation in the current work. In the future, this technique may enable many potential applications. For example, in a 3D volumetric display system, the 3D object can be usually sliced into multiple 2D images to project with SLM in a time-multiplexing way [14]. Since our method can realize high-speed 3-color holographic projection, an object can be sliced finely into several hundred images projected to different planes in sequence, and still maintain flickering-free. In adaptive optics, our method can also take advantage of its high refresh rate and realize chromatic aberration correction and multi-color wavefront shaping through a dynamic scattering medium [32,34]. In the microscopya, where the Airy beam is found to be a powerful tool for super-resolution fluorescent imaging, our method has potential to realize high-speed multi-color fluorescent imaging based on multi-color Airy beams [40]. In addition to DMD, similar ideas to this paper could be also generalized to other devices such as LC-SLM, Ferro-Electric SLM, and LCD. This superpixel method explores its full capability in multi-color complex light field modulation, paving a new door for future applications in biomedical imaging, information display, 3D holography, and optical micromanipulation.

Disclosures. The authors declare no conflicts of interest.

Data availability. Data underlying the results presented in this paper are not publicly available at this time but may be obtained from the authors upon reasonable request. Our source code can be found in Ref. [35].

References

1. D. Pi, J. Liu, and Y. Wang, "Review of computer-generated hologram algorithms for color dynamic holographic three dimensional display," Light: Sci. Appl. **11**(1), 231 (2022).
2. P. W. M. Tsang, Y. T. Chow, and T.-C. Poon, "Generation of edge-preserved noise-added phase-only hologram," Chin. Opt. Lett. **14**(10), 100901 (2016).
3. B. R. Brown and A. W. Lohmann, "Complex Spatial Filtering with Binary Masks," Appl. Opt. **5**(6), 967–969 (1966).
4. A. W. Lohmann and D. P. Paris, "Binary Fraunhofer Holograms, Generated by Computer," Appl. Opt. **6**(10), 1739–1748 (1967).
5. W.-H. Lee, "Binary Computer-generated hologram," Appl. Opt. **18**(21), 3661–3669 (1979).
6. P. M. Birch, R. Young, D. Budgett, and Chris Chatwin, "Two-pixel computer-generated hologram with a zero-twist nematic liquid-crystal spatial light modulator," Optics Letters. **25**(14), 1013–1015 (2000).
7. S. A. Goorden, J. Bertolotti, and A. P. Mosk, "Superpixel-based spatial amplitude and phase modulation using a digital micromirror device," Opt. Express **22**(15), 17999–18009 (2014).
8. You-Quan Jia, Qi Feng, Bin Zhang, Wei Wang, Cheng-You Lin, and Ying-Chun Ding, "Superpixel-Based Complex Field Modulation Using a Digital Micromirror Device for Focusing Light through Scattering Media," Chinese Phys. Lett. **35**(5), 054203 (2018).
9. E. Buckley, "Real-Time Error Diffusion for Signal-to-Noise Ratio Improvement in a Holographic Projection System," J. Disp. Technol. **7**(2), 70–76 (2011).
10. P. W. M. Tsang and T.-C. Poon, "Novel method for converting digital Fresnel hologram to phase-only hologram based on bidirectional error diffusion," Opt. Express **21**(20), 23680–23686 (2013).
11. S. Jiao, D. Zhang, C. Zhang, Y. Gao, T. Lei, and X. Yuan, "Complex-Amplitude Holographic Projection with a Digital Micromirror Device (DMD) and Error Diffusion Algorithm," IEEE J. Sel. Top. Quantum Electron. **26**(5), 8 (2020).
12. H. Nakayama, N. Takada, Y. Ichihashi, S. Awazu, T. Shimobaba, N. Masuda, and T. Ito, "Real-time color electroholography using multiple graphics processing units and multiple high-definition liquid-crystal display panels," Appl. Opt. **49**(31), 5993–5996 (2010).
13. S. Liu, Y. Li, P. Zhou, X. Li, N. Rong, S. Huang, W. Lu, and Y. Su, "A multi-plane optical see-through head mounted display design for augmented reality applications," Journal of the SID **24**(4), 246–251 (2016).
14. S. Liu, Y. Li, and Y. Su, "Multiplane displays based on liquid crystals for AR applications," Journal of the SID **28**(3), 224–240 (2020).

15. T. Shimobaba, A. Shiraki, N. Masuda, and T. Ito, "An electroholographic colour reconstruction by time division switching of reference lights," J. Opt. A: Pure Appl. Opt. **9**(7), 757–760 (2007).
16. Dapu Pi, Juan Liu, Ruidan Kang, Zhiqi Zhang, and Yu Han, "Reducing the memory usage of computer-generated hologram calculation using accurate high-compressed look-up-table method in color 3D holographic display," Opt. Express **27**(20), 28410–28422 (2019).
17. D. Pi, J. Liu, and S. Yu, "Speckleless color dynamic three-dimensional holographic display based on complex amplitude modulation," Appl. Opt. **60**(25), 7844–7848 (2021).
18. Michał Makowski, Izabela Ducin, Karol Kakarenko, Jaroslaw Suszek, Andrzej Kolodziejczyk, and Maciej Sype, "Extremely simple holographic projection of color images," Proc. SPIE **6**, 7 (2012).
19. T. Ito and K. Okano, "Color electroholography by three colored reference lights simultaneously incident upon one hologram panel," Opt. Express **12**(18), 4320–4325 (2004).
20. M. Makowski, M. Sypek, and A. Kolodziejczyk, "Colorful reconstructions from a thin multi-plane phase hologram," Opt. Express **16**(15), 11618–11623 (2008).
21. M. Makowski, M. Sypek, I. Ducin, A. Fajst, A. Siemion, J. Suszek, and A. Kolodziejczyk, "Experimental evaluation of a full-color compact lensless holographic display," Opt. Express **17**(23), 20840–20846 (2009).
22. J. Bengtsson, "Kinoforms Designed To Produce Different Fan-Out Patterns For Two Wavelengths," Appl. Opt. **37**(11), 2011–2020 (1998).
23. Y. Ogura, N. Shirai, J. Tanida, and Y. Ichioka, "Wavelength-multiplexing diffractive phase elements: design, fabrication, and performance evaluation," J. Opt. Soc. Am. A **18**(5), 1082–1092 (2001).
24. A. Jesacher, S. Bernet, and M. Ritsch-Marte, "Colour hologram projection with an SLM by exploiting its full phase modulation range," Opt. Express **22**(17), 20530–20541 (2014).
25. G. A. Siviloglou, J. Broky, A. Dogariu, and D. N. Christodoulides, "Observation of Accelerating Airy Beams," Phys. Rev. Lett. **99**(21), 213901 (2007).
26. G. Gibson, J. Courtial, M. J. Padgett, M. Vasnetsov, V. Pas'ko, S. M. Barnett, and S. Franke-Arnold, "Free-space information transfer using light beams carrying orbital angular momentum," Opt. Express **12**(22), 5448–5456 (2004).
27. T. Zhou, X. Lin, J. Wu, Y. Chen, H. Xie, Y. Li, J. Fan, H. Wu, L. Fang, and Q. Dai, "Large-scale neuromorphic optoelectronic computing with a reconfigurable diffractive processing unit," Nat. Photonics **15**(5), 367–373 (2021).
28. O. Katz, Y. Bromberg, and Yaron Silberberg, "Compressive ghost imaging," Appl. Phys. Lett. **95**(13), 131110 (2009).
29. W. Jiang, X. Li, X. Peng, and B. Sun, "Imaging high-speed moving targets with a single-pixel detector," Opt. Express **28**(6), 7889–7897 (2020).
30. Zhihao Zhou, Wei Liu, Jiajing He, Lei Chen, Xin Luo, Dongyi Shen, Jianjun Cao, Yaping Dan, Xianfeng Chen, and Wenjie Wan, "Far-field super-resolution imaging by nonlinearly excited evanescent waves," Adv. Photonics **3**(02), 025001 (2021).
31. G. Kontenis, D. Gailevicius, L. Jonušauskas, and V. Purlys, "Dynamic aberration correction via spatial light modulator (SLM) for femtosecond direct laser writing: towards spherical voxels," Optics Express. **28**(19), 27850–27864 (2020).
32. L. Wanga, W. Yana, R. Li, X. Weng, J. Zhang, Z. Yang, L. Liu, T. Ye, and J. Qu, "Aberration correction for improving the image quality in STED microscopy using the genetic algorithm," Nanophotonics **7**(12), 1971–1980 (2018).
33. I. M. Vellekoop and A. P. Mosk, "Focusing coherent light through opaque strongly scattering media," Optics Letters. **32**(16), 2309–2311 (2007).
34. S. Guo, R. Stern, H. Zhang, and L. Pang, "Speedy light focusing through scattering media by a cooperatively FPGA-parameterized genetic algorithm," Opt. Express **30**(20), 36414–36428 (2022).
35. H. Yan, Y. Sun, Y. Lin, F. Chu, and W. Wan, "Multi-color superpixel method," Github (2023), https://github.com/Hengzhe/Superpixel_DMD.
36. G. Makey, Ö. Yavuz, D. K. Kesim, A. Turnali, P. Elahi, S. Ilday, O. Tokel, and FÖ Ilday, "Breaking crosstalk limits to dynamic holography using orthogonality of high-dimensional random vectors," Nat. Photonics **13**(4), 251–256 (2019).
37. P. Yu, Y. Liu, Z. Wang, J. Liang, X. Liu, Y. Li, C. Qiu, and L. Gong, "Ultrahigh-density 3D holographic projection by scattering-assisted dynamic holography," Optica **10**(4), 481–489 (2023).
38. Rafael C. Gonzalez and Richard E. Woods, *Digital Image Processing*, (Third Edition, Pearson Education, 2017), Chapter: 4.3.
39. J. Cheng, C. Gu, D. Zhang, and S.-C. Chen, "High-speed femtosecond laser beam shaping based on binary holography using a digital micromirror device," Opt. Lett. **40**(21), 4875–4878 (2015).
40. S. Jia, J. C. Vaughan, and X. Zhuang, "Isotropic three-dimensional super-resolution imaging with a self-bending point spread function," Nat. Photonics **8**(302), 8 (2014).